IEICE TRANS. INF. & SYST., VOL.E98–D, NO.2 FEBRUARY 2015

LETTER

Multi-Orientation Log-Gabor Local Binary Pattern for Face Representation and Recognition

Cheng ZHANG[†a)], **Yuzhang GU**[†], ***Nonmembers***, **Zhengmin ZHANG**[†], ***Member***, ***and*** **Yunlong ZHAN**[†], ***Nonmember***

SUMMARY In this paper, we propose a face representation approach using multi-orientation Log-Gabor local binary pattern (MOLGLBP) for realizing face recognition under facial expressions, illuminations and partial occlusions. Log-Gabor filters with different scales (frequencies) and orientations are applied on Y, I, and Q channel image in the YIQ color space respectively. Then Log-Gabor images of different orientations at the same scale are combined to form a multi-orientation Log-Gabor image (MOLGI) and two LBP operators are applied to it. For face recognition, histogram intersection metric is utilized to measure the similarity of faces. The proposed approach is evaluated on the CurtinFaces database and experiments demonstrate that the proposed approach is effectiveness against two simultaneous variations: expression & illumination, and illumination & occlusion.

key words: *face recognition, YIQ, Log-Gabor, LBP, simultaneous variation*

1. Introduction

Generally speaking, facial feature descriptor methods can be summarized as two categories: holistic and local. Many holistic description approaches have been proposed, among which principal component analysis (PCA) [1], linear discriminant analysis (LDA) [2], independent component analysis (ICA) [3] are the typical examples. The holistic representation methods can work well with sufficient training samples. However, the recognition performance of these methods will decrease significantly under different variations with facial expressions, illuminations, and partial occlusions.

Local feature descriptors are receiving a great deal of attention because they are more robust to facial expressions, different illuminations, and partial occlusions, as opposed to holistic feature descriptors. Local binary pattern (LBP) operator generates a series of binary codes based on the signs of pixel difference with respect to its neighbors [4]. LBP is an effective way to represent faces and has computational simplicity. Gabor wavelet transformation [5], [6] has a good characterization when representing the spatial information and frequency information of the image. Zhang et al. [7] applied a set of Gabor filters on face images followed by block processing using LBP and presented a local Gabor based binary pattern histogram sequence (LGBPHS) to represent face. Lei et al. [8] proposed Gabor volume based LBP (GV-LBP) for face recognition. GV-LBP not only described the neighboring relationship in the spatial domain, but also depicted the neighboring changes during different scales and orientations. Yi et al. [9] presented a log-Gabor based feature termed Histogram of log-Gabor Magnitude Patterns (HLGMP) which adopted the bag-of-words image representation framework. These approaches generally applied a set of filters on the face image, which led to many Gabor or log-Gabor faces. Processing of these faces incurred heavy computation costs even when the image was relatively small.

Recent research demonstrates that different color spaces transformed from the RGB color space show different discriminating power for pattern recognition [10]–[12]. HSV, HSI, YUV, YCbCr, and YIQ, are the representative color spaces. Moreover, a general discriminant color model derived from the RGB color space has been shown more effective for face recognition than the original RGB color space [12]. YIQ color space is selected in the proposed approach.

As Gabor functions of arbitrarily wide bandwidth cannot be constructed and still maintain a reasonably small DC component in the even-symmetric filter, an alternative to the Gabor function is the Log-Gabor function proposed by Field [13]. Log-Gabor filters can be constructed with arbitrary bandwidth and have no DC component.

Therefore, in this paper, we present a novel face representation method, multi-orientation Log-Gabor LBP (MOLGLBP), which is not only robust to different face variations but also with much discriminating power. The major flowchart of this approach is shown in Fig. 1. Since the types of variations are unknown for a given image, it is significant for a face recognition algorithm that deals with different variations simultaneously. Most of previous studies handled one challenge at one time. Our proposed approach is largely devoted to address the problem of face recognition in the presence of two simultaneous variations: expression & illumination, and illumination & occlusion. The remaining part of the paper is organized as follows. Section 2 describes the proposed approach in detail. Section 3 focuses on experiments along with some comparisons. Finally, some conclusions are given in Sect. 4.

Manuscript received June 13, 2014.
Manuscript revised September 14, 2014.
Manuscript publicized October 27, 2014.

[†]The authors are with the Shanghai Institute of Microsystem and Information Technology, Shanghai, China.
a) E-mail: mjcheng@mail.sim.ac.cn

DOI: 10.1587/transinf.2014EDL8120

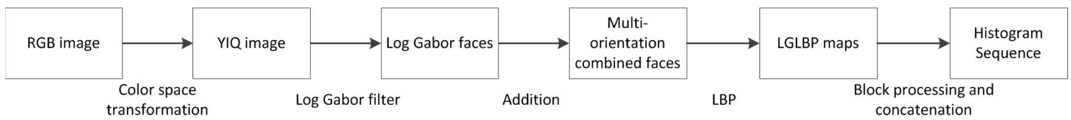

Fig. 1 The flowchart of the proposed face description approach.

Table 1 The correlation between RGB and YIQ color channels in percentage.

Channels	R	G	B	Y	I	Q
R	100	94.44	90.20	97.47	44.28	15.56
G	94.44	100	95.33	99.29	18.60	4.76
B	90.20	95.33	100	95.64	7.64	15.86
Y	97.47	99.29	95.64	100	25.21	4.23
I	44.28	18.60	7.64	25.21	100	29.61
Q	15.56	4.76	15.86	4.23	29.61	100

Fig. 2 Y, I, and Q channel image in YIQ color space.

2. Proposed Approach

2.1 YIQ Color Space

Color information is helpful for improving the performance of face recognition due to the complementary characteristics among the color component images. The R, G, and B component image in the RGB color space have large mutual information, and thus these three channel images contain a lot of redundant information. However, the color channels in YIQ color space have good independence with each other. The YIQ color space is defined as follows:

$$\begin{bmatrix} Y \\ I \\ Q \end{bmatrix} = \begin{bmatrix} 0.2989 & 0.5870 & 0.1140 \\ 0.5959 & -0.2744 & -0.3216 \\ 0.2115 & -0.5229 & 0.3114 \end{bmatrix} \begin{bmatrix} R \\ G \\ B \end{bmatrix} \quad (1)$$

Table 1 shows the average mutual information in percentage between the various color channels in RGB and YIQ color spaces for CurtinFaces database [14] using over 4000 face images. Table 1 indicates that the color channels in RGB color space are highly correlated with each other, but the color channels in YIQ color space have low mutual entropy. Moreover, Y-R, Y-G, and Y-B color channels have high correlation, which means Y channel image and RGB color space contain almost the same information. Therefore, YIQ color space contains more information than the RGB color space. Figure 2 shows the component images in the YIQ color space.

2.2 Log-Gabor Filter

Gabor filter can analyze signal local properties in different areas and shows excellent locality in both space and frequency domains. Gabor kernel has similar function with

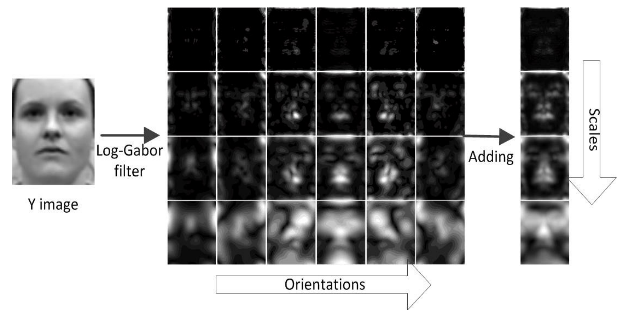

Fig. 3 The Y image is processed with Log-Gabor filters and the Log-Gabor images of six orientations at the same scale are combined into a multi-orientation Log-Gabor image.

simple cell characteristics of the visual cortex of human brains [15]. However, Gabor filter has its limitation with limited bandwidth, and it contains a small DC part. Log-Gabor filter can overcome these problems [13]. Equations related to Log-Gabor Filter are defined as follows:

$$LGF(f, angle) = LGTF(f) .* Spread(angle) \quad (2)$$

$$LGTF(f) = \exp\{-[\log(r/f)]^2/2[\log(\sigma_1)]^2\} \quad (3)$$

$$Spread(angle) = \exp\{-[F(angle)]^2/2\sigma_2^2\} \quad (4)$$

Here, *LGTF* represents Log-Gabor Gaussian transfer function in the frequency domain; *Spread* is an angular filter; $.*$ is dot product; r is the radius of the polar coordinate in the frequency plane; σ_1 is ratio of the standard deviation of Gaussian function in the frequency domain to the filter center frequency; σ_2 is the standard deviation of angular Gaussian function; *angle* is the polar angle; F is a function which makes *Spread* to be a Gaussian filter centered at the polar angle. Finally, the Log-Gabor feature of face image can be obtained by the following equation:

$$Response(f, angle) = IFFT(FFT(img) .* LGF(f, angle)) \quad (5)$$

Here, *FFT* represents fast Fourier transform; *IFFT* represents inverse fast Fourier transform; and *img* is the face image.

In this paper, we use Log-Gabor kernels at four scales $f \in \{1, 2, 3, 4\}$ and six orientations $angle \in \{1, 2, 3, 4, 5, 6\}$. σ_1 is set with 0.65. Figure 3 illustrates an example with Y image is processed with Log-Gabor filters, then the Log-Gabor face images with different orientations at the same scale are fused into one MOLGI.

2.3 Local Binary Pattern

LBP is a non-parametric operator which describes the local spatial structure of an image. Ojala et al. [16] introduced this operator and showed its high discriminative power for texture classification. In a 3×3 neighborhood of an image, the basic LBP operator assigns a binary label 0 or 1 to each surrounding pixel by thresholding the central pixel value and considers the result as a binary number:

$$LBP = \sum_{p=0}^{7} s(f_p - f_c)2^p \tag{6}$$

$$s(x) = \begin{cases} 1, x \geq 0 \\ 0, x < 0 \end{cases} \tag{7}$$

where f_c is the gray value of the center pixel c; f_p ($p = 0, 1, \ldots, 7$) is the gray value of the neighbors. Then Ojala et al. [17] developed $LBP_{P,R}$ operator that allowed LBP to deal with any size of neighborhoods by using circular neighborhoods, where P is the number of neighbors and R is the radius of the neighborhood. If the coordinate of f_c is (x, y), then the coordinate of f_p is given by $(x - R\sin(2\pi p/P), y + R\cos(2\pi p/P))$. If the coordinates of neighbors are not integers, the gray values of them are estimated by bilinear interpolation. Ojala et al. [17] also observed that most of the texture information was contained in a small subset of LBP pattern. These patterns, called uniform patterns, contain at most two bitwise 0 to 1 or 1 to 0 (circular binary code). For example, 0000000, 00011000, and 10000000 are uniform patterns. All remaining patterns are assigned with a single label. There are a total of 59 uniform patterns. After these two extensions, the extended LBP can be expressed as $LBP_{P,R}^{u2}$, where $u2$ represents the uniform patterns.

2.4 MOLGLBP Histogram Sequence

To obtain MOLGLBP histogram sequence for a face image, we first apply an LBP operator on each MOLGI and get the corresponding MOLGLBP map. Facial expressions, varying illuminations, and partial occlusions affect the robustness of face global features, but local region features can be less or not influenced by these variations. Therefore, each MOLGLBP map is spatially divided into multiple non-overlapping regions. To better describe local facial information, in this paper, both $LBP_{8,1}^{u2}$ and $LBP_{8,2}^{u2}$ are used for extracting local features from the face image. Figure 4 shows two local histograms derived from two scale LBP operators in a sub-window of a Y image. The horizontal axis presents the 59 uniform patterns. It is easy to see that the two histograms are complementary to another. So it can improve information completeness when $LBP_{8,1}^{u2}$ and $LBP_{8,2}^{u2}$ are used together. Figure 5 demostrates four MOLGLBP maps corresponding to four MOLGIs with different scales. The four maps are obtained by $LBP_{8,1}^{u2}$ operator. Finally, all the histograms extracted from the regions of all the MOLGLBP maps are concatenated into a single histogram sequence to represent the given face image. The details can be explained as follows: a histogram $\boldsymbol{h}$ of the labelled image $f(x, y)$ can be defined as

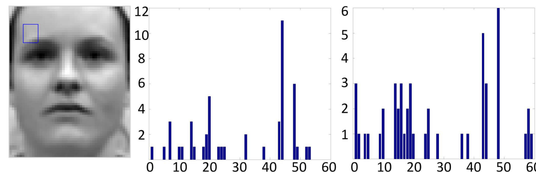

Fig. 4 A Y image and two local histograms corresponding to the two scale operators: $LBP_{8,1}^{u2}$ and $LBP_{8,2}^{u2}$ from a sub-window of 8×6 pixels.

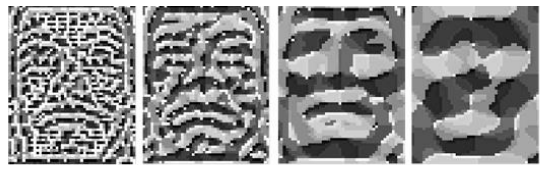

Fig. 5 Four MOLGLBP maps corresponding to four MOLGIs with different scales.

$$h_i = \sum_{x,y} I\{f(x, y) = i\} \;\; i = 0, 1, \ldots, n-1 \tag{8}$$

Here, n is the number of different labels produced by the LBP operator and $I(x) \in \{0, 1\}$ is an indication function of a Boolean condition. The histogram $\boldsymbol{h}$ is $\boldsymbol{h} = (h_1, h_2, \ldots, h_{n-1})$. The concrete processes for Y, I and Q channel image are the same. Finally, The MOLGLBP histogram sequence $\boldsymbol{H}$ is derived by concatenating three histograms $\boldsymbol{H}_1$, $\boldsymbol{H}_2$, and $\boldsymbol{H}_3$ to represent the face, where $\boldsymbol{H}_c$ ($c = 1, 2, 3$) is the specific channel image Y, I and Q, respectively.

In order to match two face images, histogram intersection metric is used as similarity measure to compare the histogram feature vectors of the two faces.

3. Experiments

3.1 Dataset

In this paper, we mainly cope up with face recognition under two simultaneous variations: expression & illumination, illumination & occlusion. Due that face images in most of face databases just contain one variation at one time, we utilize CurtinFaces database for experiments to demonstrate the effectiveness of the proposed method. CurtinFaces dataset contains over 5000 images of 52 subjects. The subset used in our experiments consists of 2132 images of 52 individuals with variations in facial expression (E), illuminations (I) and partial occlusions (O). For each subject, there are 35 images at $7E \times 5I$ and 6 images at $3I \times 2O$. Before our experiments, all the face images are cropped and normalized to the size of 64×48.

3.2 Experiments on Expression and Illumination

In this experiment, we evaluate the proposed approach against expression and illumination variations. Figure 6 shows 35 facial images of the same object. For each object, 2 images randomly selected from the 35 images compose the gallery set and the remaining 33 images compose

Table 2 The performance of different methods on facial images with simultaneous variation in expression and illumination.

Methods	PCA	LDA	LBP	LGBPHS	HLGMP	GV-LBP	Ours
Rank-1 RR(%)	68.71	71.85	72.26	85.78	86.13	86.36	88.46
VR(FAR=0.1%)	51.22	51.40	53.26	61.95	62.59	63.23	65.50

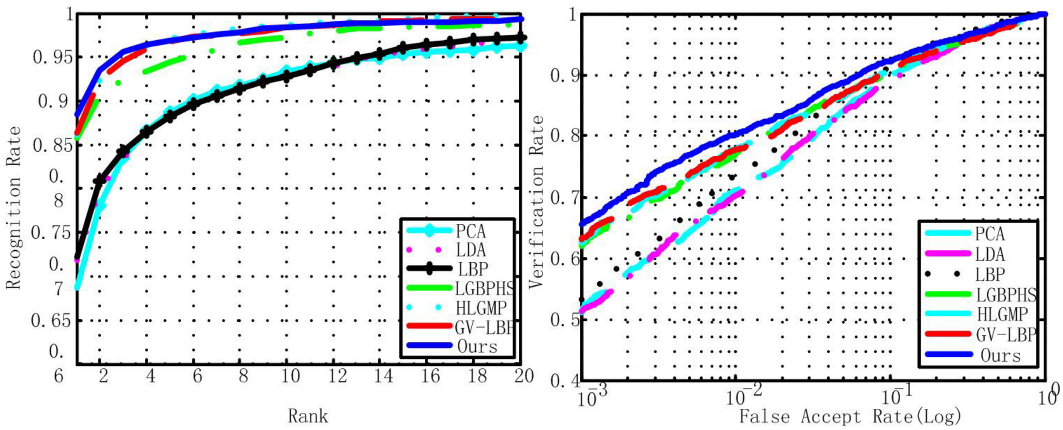

Fig. 7 The cumulative match curves and the receiving operating characteristic curves for facial images with simultaneous variation in expression and illumination.

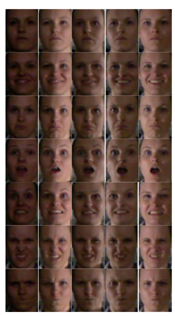

Fig. 6 35 facial images with simultaneous variation in expression and illumination.

the probe set. The experiments are carried out repeatedly 20 times and the final results are obtained from the average of these 20 results. Table 2 shows the comparison of our approach with PCA, LDA, LBP, LGBPHS, HLGMP and GV-LBP, where rank-1 RR represents rank-1 recognition rate and VR represents verification rate at the 0.1% false acceptance rate (FAR). Moreover, Fig. 7 illustrates the cumulative match curves (CMC) and the receiving operating characteristic (ROC) curves for different methods. The experiment results indicate that the proposed approach achieves much better performance than other methods of previous studies to address face recognition under simultaneous variation in expression and illumination. Moreover, Table 3 illustrates that the computation cost of our approach is greatly reduced relative to that of LGBPHS, HLGMP and GV-LBP. All the experiments are carried out using MATLAB 2012B on a 3GHz machine with 3GB RAM.

To validate that YIQ color space contains more useful information than RGB color space, we utilize RGB color space, Y channel image, and YIQ color space for comparison on the subset with simultaneous variation in expression and illumination. Table 4 illustrates the rank-1 recognition rates of different methods on these three situations. It shows Y channel image has similar performance with RGB color space and YIQ color space achieves best results among them, which demonstrates that YIQ color space can represent the face image better than the RGB color space.

Table 3 The mean time cost for recognizing one person of different methods.

Methods	LGBPHS	HLGMP	GV-LBP	Ours
Mean time (s)	0.4275	0.3556	0.5013	0.1182

Table 4 The rank-1 recognition rates of different methods with three cases in percentage.

	LGBPHS	HLGMP	GV-LBP	Ours
RGB	77.54	77.88	78.73	80.56
Y	78.32	78.85	79.45	81.33
YIQ	85.78	86.13	86.36	88.46

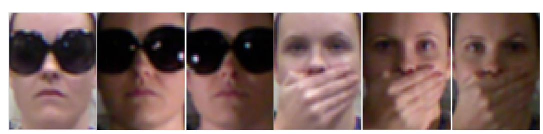

Fig. 8 6 examples of facial images with simultaneous variation in illumination and occlusion.

3.3 Experiments on Illumination and Occlusion

In this section, we test the proposed approach on facial images with simultaneous variation illumination and occlusion. Figure 8 illustrates 6 facial images of the same object. For each person, the gallery set is composed of 2 images randomly selected from the 6 images and the left 4 images compose the probe set. The experiments are performed re-

Table 5 The performance of different methods on facial images with simultaneous variation in illumination and occlusion.

Methods	PCA	LDA	LBP	LGBPHS	HLGMP	GV-LBP	Ours
Rank-1 RR(%)	56.25	55.77	62.59	74.53	74.52	74.83	76.63
VR(FAR=0.1%)	29.81	26.44	32.21	49.24	49.42	49.94	50.35

Table 6 Comparison of mean time and rank-1 RR of Gabor, Log-Gabor and MOLGI.

Methods	Gabor	Log-Gabor	MOLGI
Mean time (s)	0.4388	0.4216	0.1182
Rank-1 RR(%)	85.96	87.18	88.46

peatedly 10 times and the average results are used as the final results. Table 5 exhibits that the experiment results of the proposed approach are compared with these of PCA, LDA, LBP, LGBPHS, HLGMP and GV-LBP. The experiment results demonstrate that our approach shows more robustness than other popular methods against illumination and occlusion variations.

3.4 Comparison of Gabor, Log-Gabor and MOLGI

To evaluate the contribution of the proposed approach, we make some experiments to compare Gabor, Log-Gabor, and MOLGI methods when all other conditions are the same. The experiments are tested on the subset with simultaneous variation in expression and illumination. Table 6 shows the mean time cost for recognizing one person and rank-1 recognition rate under these three conditions. It illustrates that Gabor and Log-Gabor method has almost the same mean time cost, but MOLGI is about 4 times faster than them two. The rank-1 recognition rate of Gabor is 1.22% lower than that of Log-Gabor and MOLGI has a 1.28% higher recognition rate than Log-Gabor method. It demonstrates that the proposed approach achieves the best performance by using Log-Gabor and multi-orientation fusing in combination.

4. Conclusions

The proposed approach combines Log-Gabor filters with YIQ color space. YIQ contains more discriminative information than the RGB color space. Fusing Log-Gabor images with different orientation at the same scale reduces the computation complexity. The proposed approach was compared with PCA, LDA, LBP, LGBPHS, HLGMP and GV-LBP and shown to be superior to these methods. Experiments on the CurtinFaces database have evidently illustrated the effectiveness and robustness of MOLGLBP to two simultaneous variations: expression & illumination, and illumination & occlusion. Due that our method does not consider the situation with pose variations, more focused approach and hard work are required for further research in this area.

Acknowledgments

This work is supported by the Research on the key technology of Internet of Things for urban community safety based on video sensor networks (No. 12511501700).

References

[1] M.A. Turk and A.P. Pentland, "Face recognition using eigenfaces," Proc. IEEE Comput. Soc. Conf. Comput. Vis. Pattern Recognit., pp.586–591, Maui, HI, June 1991.
[2] P. Belhumeur, J. Hespanha, and D. Kriegman, "Eigenfaces vs. fisherfaces: Recognition using class specific linear projection," IEEE Trans. Pattern Anal. Mach. Intell., vol.19, no.7, pp.711–720, July 1997.
[3] P. Comon, "Independent component analysis — A new concept?," Signal Process., vol.36, no.3, pp.287–314, April 1994.
[4] T. Ahonen, A. Hadid, and M. Pietikainen, "Face description with local binary patterns: Application to face recognition," IEEE Trans. Pattern Anal. Mach. Intell., vol.28, no.12, pp.2037–2041, Dec. 2006.
[5] T.S. Lee, "Image representation using 2D Gabor wavelets," IEEE Trans. Pattern Anal. Mach. Intell., vol.18, no.11, pp.959–971, Oct. 1996.
[6] C.J. Liu and H. Wechsler, "Gabor feature based classification using the enhanced fisher linear discriminant model for face recognition," IEEE Trans. Image Process., vol.11, no.4, pp.467–476, April 2002.
[7] W. Zhang, S. Shan, W. Gao, and H. Zhang. "Local Gabor binary pattern histogram sequence (LGBPHS): A novel non-statistical model for face representation and recognition," Proc. IEEE Intern. Conf. Comput. Vis., pp.786–791, Oct. 2005.
[8] Z. Lei, S. Liao, R. He, M. Pietikäinen, and S. Li, "Gabor volume based local binary pattern for face representation and recognition," Proc. IEEE Intern. Conf. Automatic Face & Gesture Recognition, pp.1–6, Sept. 2008.
[9] J. Yi and F. Su, "Histogram of log-Gabor magnitude patterns for face recognition," Proc. IEEE Intern. Conf. Acoustics, Speech and Signal Processing, pp.519–523, May 2014.
[10] C. Liu, "Capitalize on dimensionality increasing techniques for improving face recognition grand challenge performance," IEEE Trans. Pattern Anal. Mach. Intell., vol.28, no.5, pp.725–737, May 2006.
[11] P. Shih and C. Liu, "Comparative assessment of content-based face image retrieval in different color spaces," Int. J. Pattern Recognition and Artificial Intelligence, vol.19, no.7, pp.873–893, Nov. 2005.
[12] J. Yang and C. Liu, "A general discriminant model for color face recognition," Proc. IEEE International Conference on Computer Vision, pp.14–20, Rio de Janeiro, Oct. 2007.
[13] D.J. Field, "Relations between the statistics of natural images and the response properties of cortical cells," J. Opt. Soc. Am., vol.4, no.12, pp.2379–2394, Dec. 1987.
[14] B.Y.L. Li, W. Liu, S. An, and A. Krishna, "Tensor based robust color face recognition," Proc. 21st International Conference on Pattern Recognition, pp.1719–1722, Tsukuba, Nov. 2012.
[15] D. Field, "What is the goal of sensory coding," Neural Computation, vol.6, no.4, pp.559–601, July 1994.
[16] T. Ojala, M. Pietikainen, and D. Harwood, "A comparative study of texture measures with classification based on featured distributions," Pattern Recognit., vol.29, no.1, pp.51–59, Jan. 1996.
[17] T. Ojala, M. Pietikainen, and T. Maenpaa, "Multiresolution gray-scale and rotation invariant texture classification with local binary patterns," IEEE Trans. Pattern Anal. Mach. Intell., vol.24, no.7, pp.971–987, July 2002.